ADVANCES IN ATMOSPHERIC SCIENCES, VOL. 30, NO. 4, 2013, 1224–1234

Impacts of Two Types of Northward Jumps of the East Asian Upper-tropospheric Jet Stream in Midsummer on Rainfall in Eastern China

LIN Zhongda* (林中达)

State Key Laboratory of Numerical Modeling for Atmospheric Sciences and Geophysical Fluid Dynamics, Institute of Atmospheric Physics, Chinese Academy of Sciences, Beijing 100029

(Received 21 May 2012; revised 21 November 2012; accepted 23 November 2012)

ABSTRACT

The East Asian upper-tropospheric jet stream (EAJS) typically jumps north of 45°N in midsummer. These annual northward jumps are mostly classified into two dominant types: the first type corresponds to the enhanced westerly to the north of the EAJS's axis (type A), while the second type is related to the weakened westerly within the EAJS's axis (type B). In this study, the impacts of these two types of northward jumps on rainfall in eastern China are investigated. Our results show that rainfall significantly increases in northern Northeast China and decreases in the Yellow River-Huaihe River valleys, as well as in North China, during the type A jump. As a result of the type B jump, rainfall is enhanced in North China and suppressed in the Yangtze River valley.

The changes in rainfall in eastern China during these two types of northward jumps are mainly caused by the northward shifts of the ascending air flow that is directly related to the EAJS. Concurrent with the type A (B) jump, the EAJS-related ascending branch moves from the Yangtze-Huai River valley to northern Northeast (North) China when the EAJS's axis jumps from 40°N to 55°N (50°N). Meanwhile, the type A jump also strengthens the Northeast Asian low in the lower troposphere, leading to more moisture transport to northern Northeast China. The type B jump, however, induces a northwestward extension of the lower-tropospheric western North Pacific subtropical high and more moisture transport to North China.

Key words: northward jump, East Asian upper-tropospheric jet stream, eastern China rainfall, Northeast Asian low, western North Pacific subtropical high

Citation: Lin, Z. D., 2013: Impacts of two types of northward jumps of the East Asian upper-tropospheric jet stream in midsummer on rainfall in eastern China. *Adv. Atmos. Sci.*, **30**(4), 1224–1234, doi: 10.1007/s00376-012-2105-9.

1. Introduction

The East Asian jet stream (EAJS) is one of the most important components of the East Asian summer monsoon system (Tao and Wei, 2006; Huang et al., 2012). The EAJS plays a crucial role in climate variations in East Asia (Liang and Wang, 1998; Lau et al., 2000; Lu, 2004; Lin and Lu, 2009; Lin et al., 2010; Park et al., 2012), the South China Sea (Wang et al., 2012) and the western North Pacific (WNP) (Wu and Chou, 2012).

The seasonal evolution of the EAJS is characterized by abrupt jumps during the boreal summer, concurrent with sudden changes in the East Asian summer monsoon. The EAJS moves northward over the East Asian continent twice during early summer (Yeh et al., 1959; Li et al., 2004). The first jump occurs in early May, and the second is in early June. The former concurs with the onset of the South China Sea summer monsoon and the latter with the mei-yu onset (Li et al., 2004).

The EAJS continues to move northward in July, and its axis moves north of 37.5°N over eastern China (110°–125°E), corresponding to the end of the mei-yu in China (Tao and Chen, 1957; Yeh et al., 1959; Dong et al., 2010a, b). In addition, the EAJS's core retreats

*Corresponding author: LIN Zhongda, zdlin@mail.iap.ac.cn

westward from the WNP toward the Asian continent during the mei-yu season (Zhang et al., 2006; Du et al., 2009).

Recently, Lin and Lu (2008) identified a northward jump over the East Asian coast in late July. This jump is clearly distinct from the aforementioned northward shifts. The EAJS's axis jumps north of 45°N at pentad 42 (25–29 July) from approximately 40°N at pentad 40 (15–19 July). Year-to-year statistics show that this northward jump is related to the end of the Baiu season in Japan. This northward jump is consistent with the disappearance of the upper-tropospheric westerly jet over Japan, corresponding to the end of the Baiu in Japan (Murakami, 1951; Suda and Asakura, 1955).

These northward jumps in midsummer are mostly classified into two dominant types (Lin and Lu, 2008). The intensity of the EAJS is enhanced and weakened with these two types of jumps. Lin (2011) proposed that the first type of jump is caused by the coupled effect of the Rossby wave that is propagated eastward along the northern edge of the Eurasian continent, originating from West Europe and the North Atlantic, and the "Pacific-Japan (PJ)" teleconnection (Nitta, 1987), induced by the positive rainfall anomaly over the tropical WNP (Lin, 2011). The second type, however, is primarily attributed to the Rossby wave propagation along the Asian subtropical jet stream in the upper troposphere.

This study continues the work of our previous studies (Lin and Lu, 2008; Lin, 2011) and addresses two questions. The first question concerns the impacts of the two types of midsummer northward jumps of the EAJS on rainfall in eastern China. In addition, increased rainfall in the tropical WNP occurs during the first type of jump (Lin, 2011). Previous work has also identified a sudden enhancement in convective activity over the WNP in late July (Ueda et al., 1995; Wu and Wang, 2001; Lu et al., 2007; Ueda et al., 2009; Wu and Chou, 2012). The second question concerns the differences between the impacts of the two types of northward jumps of the EAJS and the enhanced convection over the tropical WNP.

The text is arranged as follows. Section 2 describes the data used in this study, the selection of the two types of northward jump events of the EAJS in midsummer, and the composite method. The impacts of the two types of EAJS jumps on rainfall in eastern China are investigated in section 3. The physical processes associated with these jumps are explored in section 4. In section 5, the impact of the increased rainfall over the tropical WNP is discussed in contrast with the two types of northward jumps of the EAJS. Finally, a summary is given in section 6.

2. Data and methods

In this study, 336 station-observed daily rainfall data east of 105°E, which are derived from the National Information Center, China Meteorological Administration (CMA), during 1958–2002 are used. The atmospheric variables used in this study are from the National Centers for Environmental Prediction/National Center for Atmospheric Research (NCEP/NCAR) reanalysis data (Kalney et al., 1996) during 1958–2002, with a horizontal resolution of 2.5°×2.5°. In addition, pentad Climate Prediction Center (CPC) Merged Analysis of Precipitation (CMAP) data (Xie and Arkin, 1997) from 1979 to 2002, provided by the National Oceanic and Atmospheric Administration/Office of Oceanic and Atmospheric Research/Earth System Research Laboratory (NOAA/OAR/ESRL), Physical Sciences Division (PSD), Boulder, Colorado, USA, on their web site at http://www.esrl.noaa.gov/psd/ are used.

According to Lin and Lu (2008), the midsummer northward jumps of the EAJS can be classified into two dominant types: type A with the enhanced westerly to the north of the EAJS's axis and type B with the weakened westerly within its axis. The type A

Table 1. The two types of northward jumps of the EAJS in midsummer.

Type A (8 years)		Type B (10 years)	
Year	Pentad (Date)	Year	Pentad (Date)
1964	P41 (20–24 Jul)	1958	P38 (5–9 Jul)
1968	P44 (4–8 Aug)	1959	P45 (9–13 Aug)
1976	P41 (20–24 Jul)	1960	P40 (15–19 Jul)
1977	P41 (20–24 Jul)	1970	P41 (20–24 Jul)
1984	P42 (25–29 Jul)	1972	P42 (25–29 Jul)
1990	P41 (20–24 Jul)	1973	P37 (30 Jun–4 Jul)
1996	P42 (24–29 Jul)	1974	P41 (20–24 Jul)
1999	P41 (20–24 Jul)	1979	P45 (9–13 Aug)
		1989	P41 (20–24 Jul)
		1997	P41 (20–24 Jul)

jump includes 8 cases, and the type B jump includes 10 cases (Table 1). To highlight the evolution of precipitation associated with the EAJS's jumps, the composite analysis used here is based on jump pentads. The jump pentad, denoted as pentad 0, is defined as the pentad during which the EAJS jumps northward. The signs "−" and "+" denote prior to and after the jump, respectively.

The abrupt northward jump of the EAJS is clearly revealed during the composite seasonal evolution of the EAJS's axis (Fig. 1). Before the jump, the axis is stabilized at approximately 40°N in both jump type scenarios. The EAJS jumps northward to 55°N in the type A jump and it jumps to 50°N in the type B jump at the jump pentad. After the jump, the EAJS's axis shifts slightly southward.

As indicated by Lin (2011), the type A jump of the EAJS is significantly affected by the tropical WNP rainfall anomaly. In this study, therefore, the tropical WNP rainfall-related component is first removed by subtracting the linearly regressed component of the WNP summer monsoon index (WNPSMI) during late June-late August from 1958–2002. The WNPSMI is defined as the difference in pentad zonal winds at 850 hPa averaged over the regions between 5°–15°N, 100°–130°E and 20°–30°N, 110°–140°E, following the method of Wang et al. (2001). The period of late June-late August, which includes 14 pentads from pentad 35 to 48, is selected because the northward jumps of the EAJS are only observed during this period. The total number of pentads used is 630 pentads (45 years multiplied by 14 pentads per year) during the years 1958–2002.

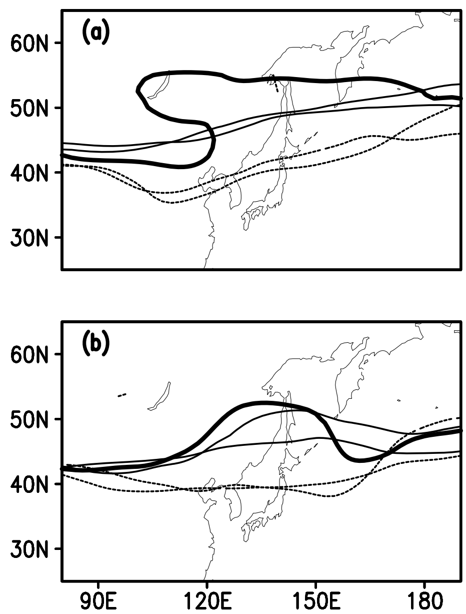

Fig. 1. Movement of the axes of the East Asian upper-tropospheric jet stream (EAJS) for the type A (a) and B (b) northward jumps of the EAJS in midsummer. The thin dashed (solid) lines signify the two pentads before (after) the northward jump, and the thick solid line indicates the pentad of northward jump.

To highlight the impacts of the northward jumps of the EAJS, the difference between the jump pentad and the period before the jumps (pentad −2 and pentad −1) is calculated. The WNPSMI-related component is first removed for this calculation, and a Student t-test is applied as a significance test of the anomalies. The two pentads before the jump are used because the EAJS's axis is stabilized at approximately 40°N at both pentad −2 and pentad −1. Pentad 0 is used in comparison to pentads −2 and −1 because the most significant northward shift in the EAJS occurs at this pentad, which is referred to as the jump pentad (Fig. 1).

To confirm the composite results, an identical analysis is performed on the data, with the linearly regressed component related to the WNP rainfall anomaly removed by using the CMAP precipitation data during 1979–2002. The WNP rainfall anomaly is depicted as the average rainfall over the region (10°–20°N, 115°–155°E) in cases where rainfall changed significantly during the type A jump (Lin, 2011). The correlation of the WNP rainfall anomaly with the WNPSMI during the 336 pentads (24 years multiplied by 14 pentads per year) from 1979 to 2002 is 0.87, which is significant at the confidence level of 99%, indicating that the WNPSMI is an appropriate way to depict the tropical WNP rainfall anomaly. The composite results are similar to those found after removing the WNPSMI-related component. Note that the CMAP precipitation data are only available starting in 1979 and that there are only 4 (3) jumps out of a total of 8 (10) jump events that are categorized as type A (B) jumps. To obtain better significance, only the results obtained after subtracting the linearly regressed component against the WNPSMI during 1958–2002 are presented.

3. Impacts on rainfall in eastern China

Figure 2 shows the evolution of composite rainfall in eastern China during the two pentads before both types of EAJS jumps and the two pentads after the jumps. The rainy belt is centered over the Yellow River-Huaihe River valleys in eastern China prior to the type A jump, though there is also strong rainfall in Southwest China along the upper reaches of the Yangtze River. One pentad later (pentad −1), the rainy belt shifts slightly northward. At the jump pen-

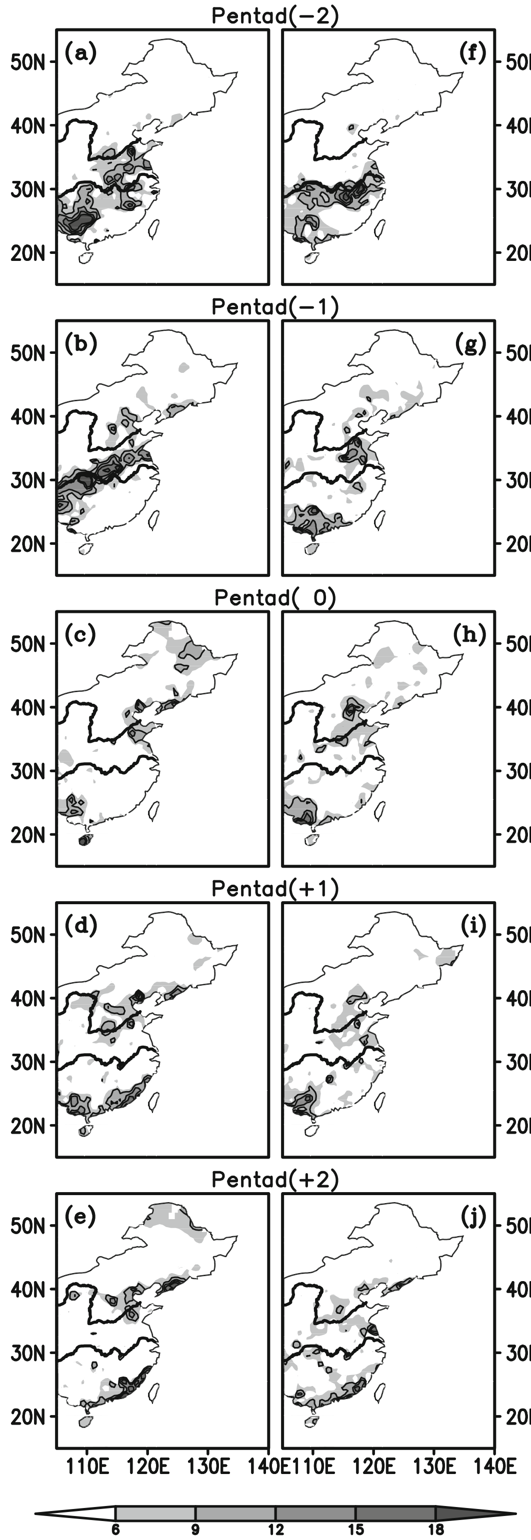

Fig. 2. Evolution of rainfall (unit: mm d^{-1}) in eastern China from two pentads before to two pentads after the type A (left panels, a–e) and B (right panels, f–j) jumps. Pentad 0 denotes the northward jump pentad, and minus and plus represent before and after the jump pentad, respectively.

tad (pentad 0), the rainy belt quickly moves northward to North and Northeast China. After the jump, the rainy belt becomes stable in North and Northeast China at pentads +1 and +2, concurrent with the appearance of another rainy belt along the southeast coast of China. Before the type B northward jump, the rainy belt moves from the Yangtze River valley at pentad −2 to the Yellow River-Huaihe River valleys at pentad −1. The rainy belt moves into North China at pentad 0 and remains in North China after the jump. There is also a clear rainy belt along the south and southwest coast of China that persists before and after the northward jump.

The changes in rainfall during the two types of jumps are more clearly revealed by the difference between the average rainfall during the two pentads before the northward jump (pentads −2 and −1) and that at the jump pentad (Fig. 3). Note that the WNPSMI-related component is removed prior to this rainfall analysis (details in section 2). Rainfall significantly decreases in the Yellow River-Huaihe River valleys, in the upper reaches of the Yangtze River valley, and in North China (Fig. 3a) during the type A jump. This reduction in rainfall is consistent with the observed northward shift of the rainy belt from between the Yangtze River valley and North China to North and Northeast China, as shown in Figs. 2a–c.

During the type B jump, rainfall increases in North China and decreases in the Yangtze River valley (Fig. 3b). This change in rainfall is in good agreement with the northward shift of the rainy belt from the Yangtze River valley to North China (Figs. 2f–h). Compared with those in the type A jump, the rainfall changes in eastern China are weaker during the type B jump. In addition, relative to the rainfall changes during the type B jump, rainfall resulting from the type A jump is significantly enhanced in northern Northeast China and suppressed in the Yellow River-Huaihe River valleys, in the upper reaches of the Yangtze River valley, and in North China (Fig. 3c).

4. Impacts of circulation changes in the Asia-Pacific region

In this section, the physical processes responsible for the rainfall changes in eastern China during the two types of EAJS jumps are investigated. This analysis is based on the change in vertical motion described in subsection 4.1 and the change in lower-tropospheric circulation and its impact on moisture transport, as described in subsection 4.2. Note that the impact of the tropical WNP rainfall anomaly is first removed in this section in order to isolate the circulation changes related to the two types of northward jumps of the

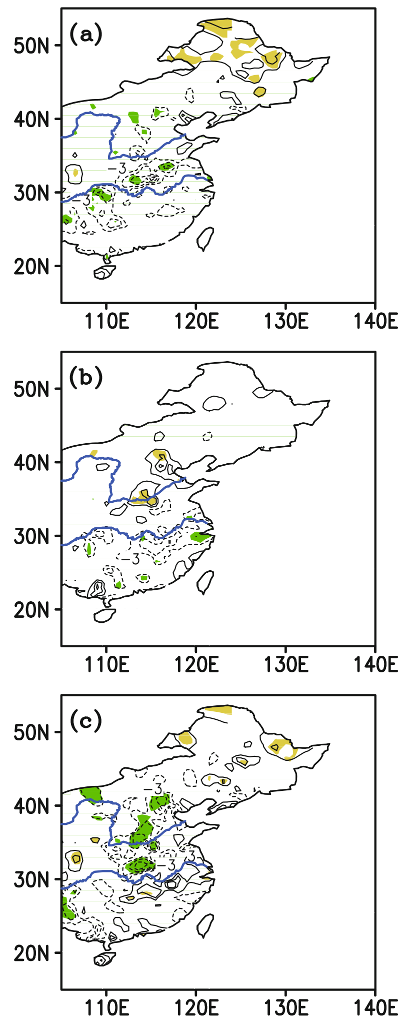

Fig. 3. (a) Composite difference in rainfall between the jump pentad (pentad 0) and the two pentads before the jump (pentads −2 and −1) for the type A jump. (b) Same as (a) but for the type B jump. (c) Difference between (a) and (b). Shading denotes significant rainfall anomaly at the confidence level of 95% in (a–b) and 90% in (c) by Student *t*-test.

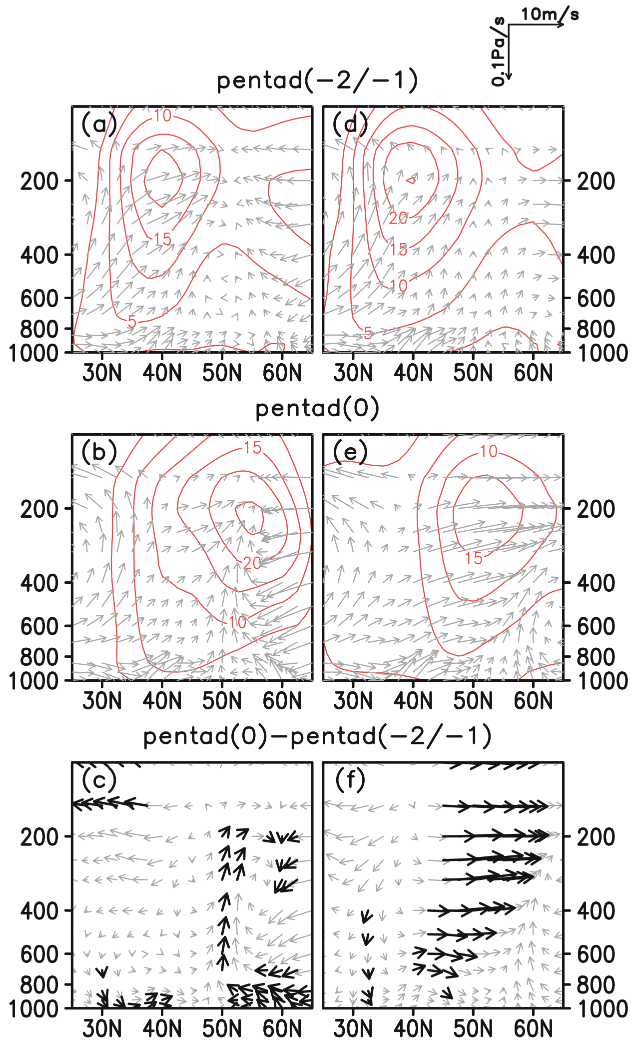

Fig. 4. Composite meridional wind and vertical velocity averaged over 110°–130°E before the jump (averages of pentad −2 and −1) (a), at the jump pentad (b), and their difference (c) for the type A jump. The vertical coordinate is pressure with units of hPa. Contours in (a–b) depict composite zonal winds averaged between 120°–150°E, which demonstrate the abrupt northward jump of the EAJS, and the dark black vector in (c) denotes significant meridional wind or vertical velocity anomalies at the 95% confidence level by Student *t*-test. (d–f) Same as (a–c) but for the type B jump.

EAJS.

4.1 *Change in vertical motion crossing the EAJS*

Figure 4 shows a vertical cross-section of the meridional wind and the vertical velocity in the meridional direction along the East Asian coast during the two types of northward jumps of the EAJS. Clearly, the northward shift of ascending motion south of the EAJS's axis is identified, concurrent with the type A (B) northward jump of the EAJS's axis from 40°N to 55°N (50°N). Prior to these northward jumps, the ascending motion directly related to the EAJS is coupled with subtropical meridional monsoon circulation. This strong ascending motion is located over the region between 30°N and 40°N to the south of the EAJS's axis, with a center at approximately 30°N over the Yangtze-Huai River valley.

The ascending motion over the East Asian coast is divided into two branches: the branch over approximately 30°N that is related to monsoon circulation and the one at approximately 50°N (40°N) that is directly associated with the EAJS during the type A

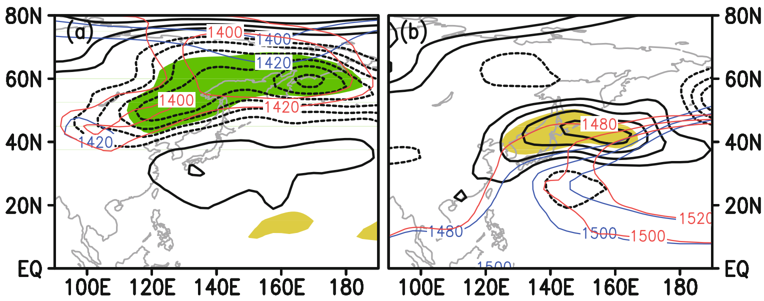

Fig. 5. (a) Composite 850-hPa geopotential height before the jump (blue contours), at the jump pentad (red contours), and their difference (black contours) for the type A jump. Contour intervals for black contours are 10 gpm, and zero contours are omitted. Shading denotes significant 850-hPa geopotential height anomalies at the 95% confidence level. (b) Same as (a) but for the type B jump.

(B) jump. Accordingly, the northward shifts of EAJS-related ascending motion cause an increase in rainfall in northern Northeast China at approximately 50°N during the type A jump and in North China at approximately 40°N during the type B jump. In addition, the weakened ascending motion to the south of 40°N leads to a reduction in rainfall in the Yellow River-Huaihe River valleys and a slight reduction in rainfall in North China during the type A jump and a reduction in rainfall in the Yangtze-Huai River valley during the type B jump.

4.2 *Changes in the Northeast Asian low and in the WNP subtropical high*

Inland rainfall depends on moisture transport, as well as on ascending motion. Previous studies have addressed the importance of southerly monsoon winds on moisture transport along eastern China (Chen and Huang, 2007; Huang and Chen, 2010). In the lower troposphere, southerly monsoon winds are determined by the zonal contrast of the geopotential height over the subtropical WNP and that over inland Asia (Guo, 1983; Shi and Zhu, 1996; Zhao and Zhou, 2005). Namely, these monsoon winds are determined by the contrast between the WNP subtropical high and the low pressure in the eastern Asia. In this section, changes in the eastern Asian low and the WNP subtropical high and their impact on rainfall in eastern China during the two types of northward jumps of the EAJS are discussed.

Figure 5 shows the composite geopotential height at 850 hPa during the two types of northward jumps of the EAJS. During the type A jump, the geopotential height is significantly reduced over the regions from Northeast Asia, northeastward through the Okhotsk Sea, to the Bering Sea. The climatological Northeast Asian low is therefore further strengthened, with the center value falling to less than 1400 gpm at the jump pentad from approximately 1420 gpm before the jump (Fig. 5a). The enhanced Northeast Asian low is attributed to the nearly barotropic cyclonic anomaly in the upper troposphere over the area east of Siberia, accompanied by a strong westerly anomaly in the upper troposphere at approximately 60°N over the Okhotsk Sea (Fig. 6a), to the north of the climatological EAJS's axis (Fig. 7a). Corresponding to the enhanced Northeast Asian low, the strong lower-tropospheric southwesterly anomaly over Northeast China (Fig. 6b), to the east of the Northeast Asian low, intensifies the climatological *in-situ* southwesterly (Fig. 7b). This intensified southwesterly over Northeast China transports more moisture to northern Northeast China, causing an increase in rainfall (Fig. 3a).

During the type B jump, the geopotential heights at 850 hPa are remarkably higher over the WNP north of Japan and slightly lower to the south over the subtropical WNP (Fig. 5b). The changes in 850-hPa geopotential height contribute to the northwestward extension of the WNP subtropical high as the 1480-gpm contour moves northwestward across Japan, the Korean Peninsula, and the Sea of Japan. Meanwhile, the ridge of the WNP subtropical high reaches approximately 40°N at the jump pentad, compared to its position at 30°N before the jump. The changes in the WNP subtropical high are associated with an anticyclonic anomaly (Fig. 6c) to the north of the EAJS's axis (Fig. 7a) and a cyclonic anomaly to the south in the upper troposphere. These anomalies are caused by the weakened EAJS during the type B jump. The southwesterly anomaly in the lower troposphere (Fig. 6d), to the west of the northwestward extension of the WNP subtropical high, intensifies the climatological southerly along eastern China toward North China (Fig. 7b). This intensified southerly along east-

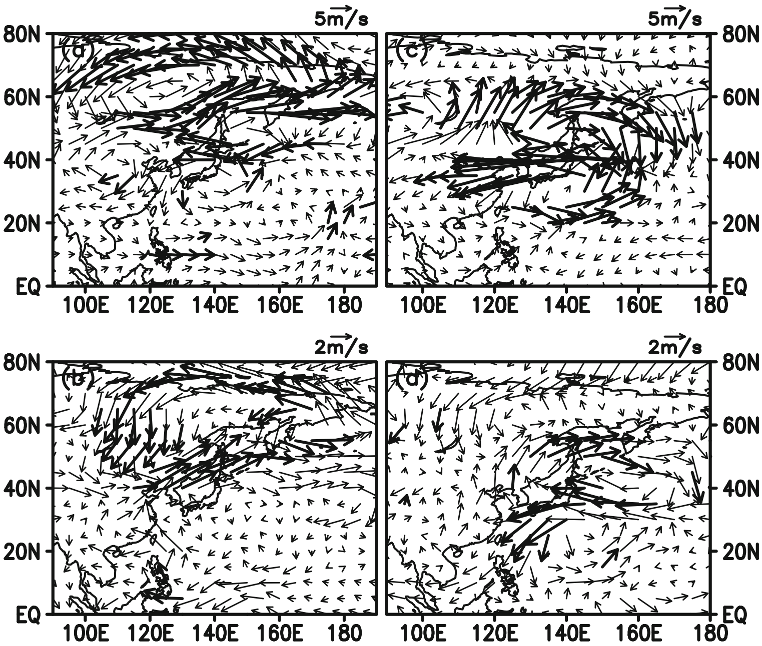

Fig. 6. Same as Figs. 4c and f but for the composite difference in horizontal winds at 200 hPa (a, c) and 850 hPa (b, d). The left panels are for the type A jump and the right panels for the type B jump. Dark black vectors denote significant zonal or meridional wind anomalies at the 95% confidence level by Student t-test.

ern China transports more moisture and contributes to increased rainfall in North China, as shown in Fig. 3b. In addition, the northeasterly anomaly to the west of the cyclonic anomaly opposes the climatological southerly (Fig. 7b) and diverges over the Yangtze River valley from the southwesterly anomaly to the north. Rainfall is reduced in the Yangtze River valley (Fig. 3b).

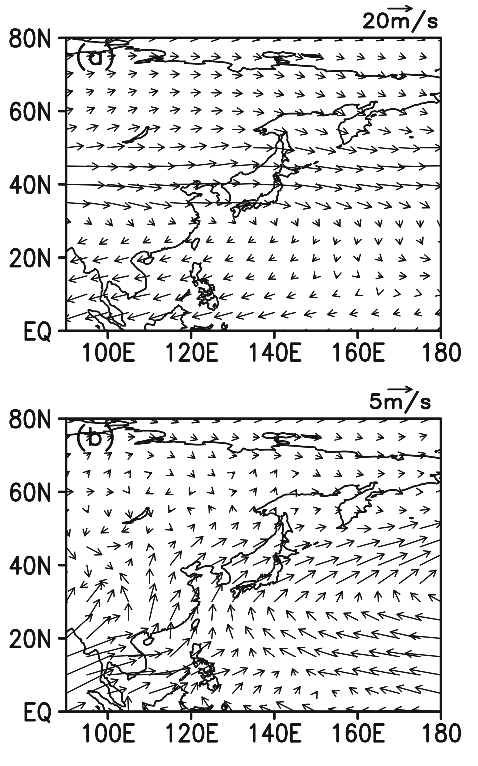

Fig. 7. Climatology of horizontal winds at 200 hPa (a) and 850 hPa (b) averaged during late June-late August from the years 1958 to 2002.

5. Impact of increased rainfall in the tropical WNP

Lin (2011) revealed that during the type A jump of the EAJS, rainfall in the tropical WNP is enhanced. Many other studies have also emphasized the impact of intraseasonal variations of the tropical WNP convective anomaly on rainfall in eastern China (e.g., Huang and Sun, 1994; Yang et al., 2010). To illustrate the effect of WNP rainfall, the WNPSMI-related pentad CMAP precipitation anomalies in late June-late August during 1979–2002 and observational station rainfall anomalies in eastern China during 1958–2002 are presented in Fig. 8. The WNPSMI was shown to be an appropriate representation of WNP rainfall variations in section 2 of this study. When the WNPSMI is positive, rainfall is enhanced in the tropical WNP, as well as in the South China Sea, and rainfall is suppressed

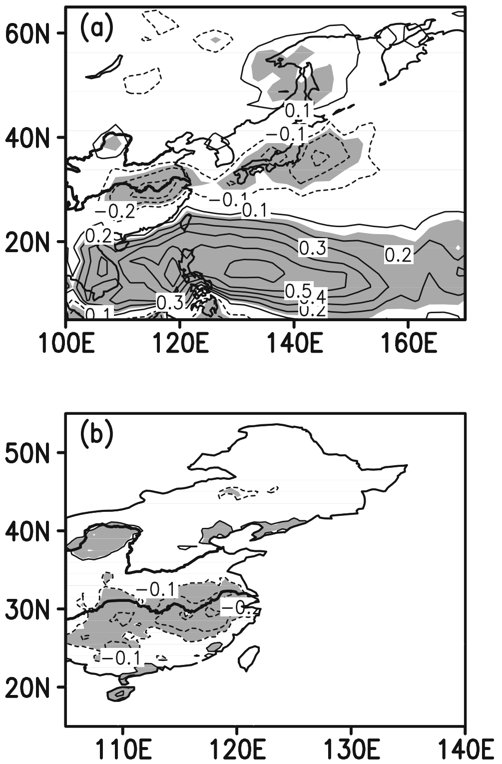

Fig. 8. (a) Correlation of pentad CMAP precipitation during late June-late August (14 pentads from pentad 35 to 48) from 1979 to 2002 with the western North Pacific summer monsoon index (WNPSMI), which is defined as the difference of zonal winds at 850 hPa averaged over the regions between (5°–15°N, 100°–130°E) and (20°–30°N, 110°–140°E), as in Wang et al. (2001). Shading denotes significant correlation at the 95% confidence level. (b) Same as (a), but for the correlation of pentad station rainfall in eastern China with the WNPSMI from 1958 to 2002.

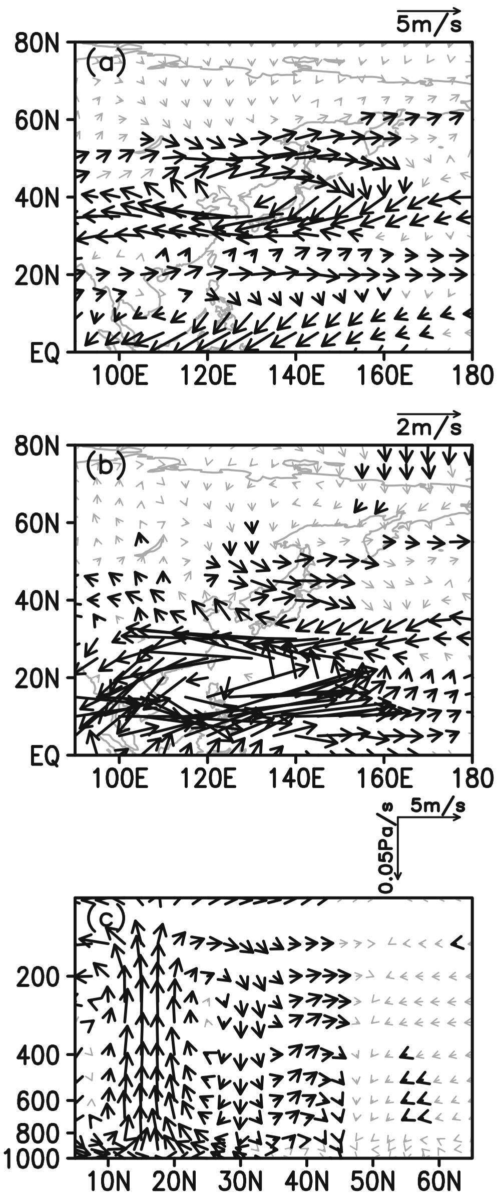

Fig. 9. The same as Fig. 8b, but for regressed pentad horizontal wind anomalies at 200 hPa (a), 850 hPa (b), and meridional winds and vertical velocity anomalies averaged between 110°E and 130°E (c). Dark black vectors denote significant anomalies at the 95% confidence level.

along the subtropical East Asian rainy belt from the Yangtze River-Huaihe River valleys, northeastward through Japan, to the WNP east of Japan. Rainfall also slightly increases west of North China. The impact of the WNPSM on rainfall in eastern China is confirmed by the WNPSMI-related station rainfall (Fig. 8b).

The increased rainfall in the tropical WNP during the type A jump revealed by Lin (2011) thus results in significantly decreased rainfall in the Yangtze-Huai River valley. In the final portion of this section, the circulation anomalies associated with the WNPSM, in contrast with those due to the northward jumps of the EAJS, are further explored.

When rainfall in the tropical WNP increases, a local anticyclonic anomaly in the upper troposphere (Fig. 9a) and a cyclonic anomaly in the lower troposphere (Fig. 9b) are observed. The northeasterly anomaly to the west of the lower-tropospheric cyclonic anomaly suppresses moisture transport to the Yangtze-Huai River valley. The circulation anomalies related to the tropical WNP rainfall include an anomalous meridional overturning circulation in the vertical cross-section over the WNP and East Asia, with a branch of ascending motion in the tropical WNP between 10°N and 20°N and a subsidence branch at approximately 30°N over the Yangtze-Huai River valley (Fig. 9c). The suppressed lower-tropospheric moisture transport and anomalous subsidence both lead to a reduction in rainfall in the Yangtze-Huai River valley. In addition, an anomalous ascending motion is also observed over 40°N, consistent with a weak increase in rainfall in North China (Fig. 8). Over East Asia, a significant upper-tropospheric westerly anomaly appears to be centered at approximately 50°N, to the north of the EAJS's axis, and an easterly anomaly between 35°N and 40°N is observed to the south of the EAJS's axis (Fig. 9a). Accordingly, the EAJS tends to shift northward, consistent with the conclusion that the increased rainfall in the tropical WNP contributes to the type A jump (Lin, 2011).

6. Conclusions

The impacts of the two types of northward jumps of the EAJS on rainfall in eastern China are investigated in this study by using daily NCEP/NCAR reanalysis data and observational station rainfall in China during 1958–2002. Rainfall is significantly enhanced in northern Northeast China and weakened in the Yellow River-Huaihe River valleys, as well as in North China, during the type A northward jump. When the EAJS is enhanced in the northern portion of the EAJS's axis. During the type B jump, the westerly is significantly weakened in the EAJS's axis, and rainfall increases in North China and decreases in the Yangtze River valley.

These changes in rainfall during the two types of jumps are primarily caused by northward shifts in ascending motion that are directly related to the EAJS. During the type A (B) jump, the EAJS-related ascending branch to the south of its axis moves from the Yangtze-Huai River valley to northern Northeast (North) China when the EAJS's axis jumps from 40°N to 55°N (50°N). Increased rainfall is observed in northern Northeast (North) China during the type A (B) jump of the EAJS. The northward shift of EAJS-related ascending motion, on the other hand, leads to decreased rainfall in the Yellow River-Huaihe River (Yangtze River) valleys during the type A (B) jump.

In addition, the associated lower-tropospheric circulation anomaly further enhances the impact of the type A (B) jump on northern Northeast China (North China) rainfall. During the type A jump, the barotropic cyclonic anomaly to the northwest of the enhanced westerly intensifies the lower-tropospheric Northeast Asian low, leading to more moisture transport to northern Northeast China and enhanced rainfall. The barotropic anticyclonic anomaly north of the weakened westerly contributes to the northwestward extension of the WNP subtropical high, increased moisture transport to North China and strengthened rainfall during the type B jump.

The impacts of the two types of northward jumps of the EAJS are compared with those related to tropical WNP rainfall. When rainfall increases in the tropical WNP, rainfall in the Yangtze-Huai River valley is significantly reduced. These changes in rainfall are due to the eastward retreat of the WNP subtropical high, which is a Rossby wave response to the tropical WNP rainfall-induced heat release, in contrast with the enhanced Northeast Asian low during the type A jump and the northwestward extension of the WNP high during the type B jump.

The enhanced rainfall in the tropical WNP during the type A jump thus results in weakened rainfall in the Yangtze-Huai River valley. Note that the type A EAJS jump causes rainfall increase in northern Northeast China and rainfall decrease in the Yellow River-Huaihe River valleys. Accordingly, the combined effect of the tropical WNP rainfall and the type A northward jump of the EAJS in midsummer leads to decreased rainfall in regions along eastern China, from the Yangtze River valley northward to North China, and increased rainfall in northern Northeast China.

Acknowledgements. The author would like to thank two anonymous reviewers for their valuable comments, which greatly improved the manuscript. The author also thanks Drs. LU Riyu and CHEN Wei from LASG, Institute of Atmospheric Physics for discussion on the impact of tropical western North Pacific rainfall and for improving the revised manuscript. This research work was supported by the National Natural Science Foundation of China (Grant No. 40905025), GYHY201006019, and GYHY200906017.

REFERENCES

Chen, J. L., and R. H. Huang, 2007: The comparison of climatological characteristics among Asian and Australian monsoon subsystems. Part II: Water vapor transport by summer monsoon. *Chinese J. Atmos. Sci.*, **31**, 766–778. (in Chinese)

Dong, L. N., P. W. Guo, P. X. Wang, and L. Qi, 2010a: Impacts of the variation of westerly jets over East Asian in July on the precipitation of East China. *Plateau Meteorology*, **29**, 286–296. (in Chinese)

Dong, L. N., P. W. Guo, and F. Y. Zhang, 2010b: Relationship between variations of East Asian subtropical westerly jet from early summer to mid summer an withdrawal of mei-yu from Jianghuai region. *Transactions of Atmospheric Sciences*, **33**, 74–81. (in Chinese)

Du, Y., Y. C. Zhang, and Z. Q. Xie, 2009: Location variation of the East Asia subtropical westerly jet and its effect on the summer precipitation anomaly over eastern China. *Chinese J. Atmos. Sci.*, **33**, 581–592. (in Chinese)

Huang, R. H., and F. Y. Sun, 1994: Impact of the convective activities over the western tropical Pacific warm pool on the intraseasonal variability of the East Asian summer monsoon. *Chinese J. Atmos. Sci.*, **18**, 456–465. (in Chinese)

Huang, R. H., and J. L. Chen, 2010: Characteristics of the summertime water vapor transports over the eastern part of China and those over the western part of China and their difference. *Chinese J. Atmos. Sci.*, **34**, 1035–1045. (in Chinese)

Huang, R. H., J. L. Chen, L. Wang, and Z. D. Lin, 2012: Characteristics, processes, and causes of the spatio-temporal variabilities of the East Asian monsoon system. *Adv. Atmos. Sci.*, **29**(5), 910–942, doi: 10.1007/s00376-012-2015-x.

Guo, Q. Y., 1983: The summer monsoon index in East Asia and its variation. *Acta Geographica Sinica*, **38**, 208–217. (in Chinese)

Kalney, E., and Coauthors, 1996: The NCEP/ NCAR 40-year reanalysis project. *Bull. Amer. Meteor. Soc.*, **77**, 437–471.

Lau, K. -M., K. -M. Kim, and S. Yang, 2000: Dynamical and boundary forcing characteristics of regional components of the Asian summer monsoon. *J. Climate*, **13**, 2461–2482.

Li, C., J. Wang, S. Lin, and H. Cho, 2004: The relationship between East Asia summer monsoon activity and northward jump of the upper westerly jet location. *Chinese J. Atmos. Sci.*, **28**, 641–658. (in Chinese)

Liang, X., and W. Wang, 1998: Associations between China monsoon rainfall and tropospheric jets. *Quart. J. Roy. Meteor. Soc.*, **124**, 2597–2623.

Lin, Z. D., 2011: Dynamical processes of two types of northward jumps of the East Asian upper-tropospheric jet stream in mid summer. *Chinese J. Atmos. Sci.*, **35**, 631–644. (in Chinese)

Lin, Z. D, and R. Y. Lu, 2008: Abrupt northward jump of the East Asian upper-tropospheric jet stream. *J. Meteor. Soc. Japan*, **86**, 857–866.

Lin, Z. D., and R. Y. Lu, 2009: The ENSO's effect on the eastern China rainfall in the following early summer. *Adv. Atmos. Sci.*, **26**, 333–342, doi: 10.1007/s00376-009-0333-4.

Lin, Z. D., R. Y. Lu, and W. Zhou, 2010: Change in early-summer meridional teleconnection over the western North Pacific and East Asia around the late 1970s. *Int. J. Climatol.*, **30**, 2195–2204.

Lu, R. Y., 2004: Associations among the components of the East Asian summer monsoon system in the meridional direction. *J. Meteor. Soc. Japan*, **82**, 155–165.

Lu, R. Y., H. Ding, C. S. Ryu, Z. D. Lin, and H. L. Dong, 2007: Midlatitude westward propagating disturbances preceding intraseasonal oscillations of convection over the subtropical western North Pacific during summer. *Geophys. Res. Lett.*, **34**, L21702, doi: 10.1029/2007GL031277.

Murakami, T., 1951: On the study of the change of the upper westerlies in the last stage of Baiu season (rainy season in Japan). *J. Meteor. Soc. Japan*, **29**, 162–175.

Nitta, T., 1987: Convective activities in the tropical western Pacific and their impact on the Northern Hemisphere summer circulation. *J. Meteor. Soc. Japan*, **70**, 243–256.

Park, J.-K., R. Y. Lu, C. F. Li, and E. B. Kim, 2012: Interannual variation of tropical night frequency in Beijing and associated large-scale circulation background. *Adv. Atmos. Sci.*, **29**, 295–306, doi: 10.1007/s00376-011-1141-1.

Shi, N., and Q. G. Zhu, 1996: An abrupt change in the intensity of the East Asian summer monsoon index and its relationship with temperature and precipitation over East China. *Int. J. Climatol.*, **16**, 757–764.

Suda, K., and T. Asakura, 1955: A study on the unusual "Baiu" season in 1954 by means of Northern Hemisphere upper air mean charts. *J. Meteor. Soc. Japan*, **33**, 233–244.

Tao, S. Y., and L. X. Chen, 1957: Atmospheric circulation structure over the Asian continent in summer. *Acta Meteorologica Sinica*, **28**, 234–246. (in Chinese)

Tao, S. Y., and J. Wei, 2006: The westward, northward advance of the subtropical high over the west Pacific in summer. *Journal of Applied Meteorological Sciences*, **17**, 513–525. (in Chinese)

Ueda, H., T. Yasunari, and R. Kawamura, 1995: Abrupt seasonal change of large-scale convective activity over the western Pacific in the northern summer. *J. Meteor. Soc. Japan*, **73**, 795–809

Ueda, H., M. Ohba, and S. P. Xie, 2009: Important Factors for the development of the Asian-northwest Pacific summer monsoon. *J. Climate*, **22**, 649–669.

Wang, B., R. Wu, and K.-M. Lau, 2001: Interannual variability of the Asian summer monsoon: Contrasts between the Indian and the western North Pacific-East Asia monsoons. *J. Climate*, **14**, 4073–4090.

Wang, X., W. Zhou, C. Y. Li, and D. X. Wang, 2012: Effects of the East Asian summer monsoon on tropical cyclone genesis over the South China Sea on an interdecadal time scale. *Adv. Atmos. Sci.*, **29**, 249–262, doi: 10.1007/s00376-011-1080-x.

Wu, R., and B. Wang, 2001: Multi-stage onset of the summer monsoon over the western North Pacific. *Climate Dyn.*, **17**, 277–289.

Wu, C., and M. Chou, 2012: Upper tropospheric forcing on late-July monsoon transition in East Asia and western North Pacific. *J. Climate*, **25**, 3929–3941.

Xie, P., and P. A. Arkin, 1997: Global precipitation: A 17-year monthly analysis based on gauge observations, satellite estimates, and numerical model outputs. *Bull. Amer. Meteor. Soc.*, **78**, 2539–2558.

Yang, J., B. Wang, B. Wang, and Q. Bao, 2010: Biweekly and 21–30-day variations of the subtropical summer monsoon rainfall over the lower reach of the Yangtze River basin. *J. Climate*, **23**, 1146–1159.

Yeh, D., S. Tao, and M. Li, 1959: The abrupt change of circulation over Northern Hemisphere during June and October. *The Atmosphere and Sea in Motion*, Rockefeller Institute Press, 249–267.

Zhang, Y., X. Kuang, W. Guo, and T. Zhou, 2006: Seasonal evolution of the upper-tropospheric westerly jet core over East Asia. *Geophys. Res. Lett.*, **33**, L11708, doi: 10.1029/2006GL026377.

Zhao, P., and Z. J. Zhou, 2005: East Asian subtropical summer monsoon index and its relationships to rainfall. *Acta Meteorologica Sinica*, **63,** 933–941. (in Chinese)